

Supplemental Information

Monocyte upregulation of podoplanin during early sepsis induces complement inhibitor release to protect liver function

Zhanli Xie¹, Bojing Shao², Christopher Hoover^{2,5}, Michael McDaniel²
Jianhua Song², Miao Jiang¹, Zhenni Ma¹, Fei Yang¹, Jingjing Han¹, Xia Bai^{1,3,4}, Changgeng
Ruan^{1,3,4}, Lijun Xia^{2,1,3,5}

Corresponding author: Lijun Xia, M.D., Ph.D., Cardiovascular Biology Research Program,
Oklahoma Medical Research Foundation, 825 N.E. 13th Street, Oklahoma City, OK 73104.
Phone: 405-271-7892. Fax: 405-271-3137. Email: lijun-xia@omrf.org

This PDF file includes:

Method
References
Supplemental Figs. 1 to 15

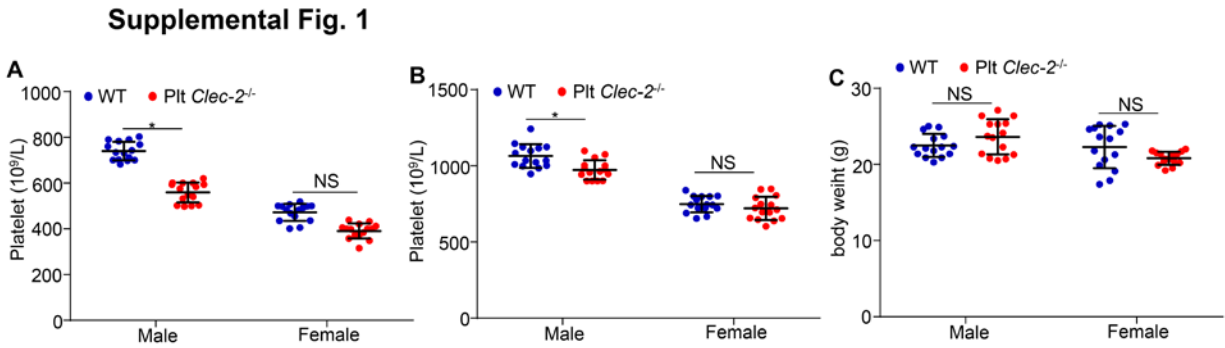
Method

Isolation of monocytes from mice. Anti-coagulated mouse blood was collected via cardiac puncture and was diluted (1:1) with Dulbecco's PBS without calcium and magnesium. Mouse monocytes are defined as CD11b^{high} (CD90/B220/CD49b/NK1.1/Ly6G/Ter-119)^{low} (1, 2). Collect mononuclear cells by Ficcol gradient centrifugation at 400g for 30min. Add antibody mix containing PE-labeled B220 (CD45R), CD49b, CD90, Ly6G, NK1.1 and Ter-119, and incubate for 10min at room temperature. After wash with PBS (2mM EDTA, 2% FBS), the cells are magnetically labeled with Anti PE Mcirobeads (4°C, 15min). The cell suspension was loaded on a MACS Column which is placed in the magnetic field of a MACS Separator. The magnetically labeled cells are absorbed in the column while the unlabeled cells run through. Collect the unlabeled cells and labeled with APC-labeled CD11b.

References:

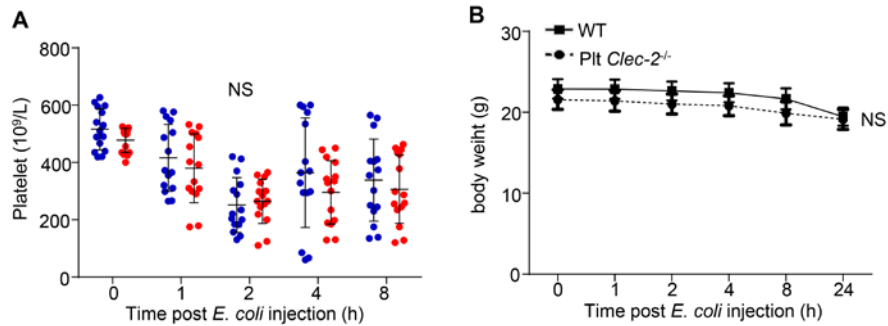
1. Swirski FK, et al. Identification of splenic reservoir monocytes and their deployment to inflammatory sites. *Science*. 2009;325(5940):612-6.
2. Yang A, et al. An essential role of high-molecular-weight kininogen in endotoxemia. *J Exp Med*. 2017;214(9):2649-70.

Supplemental Figures



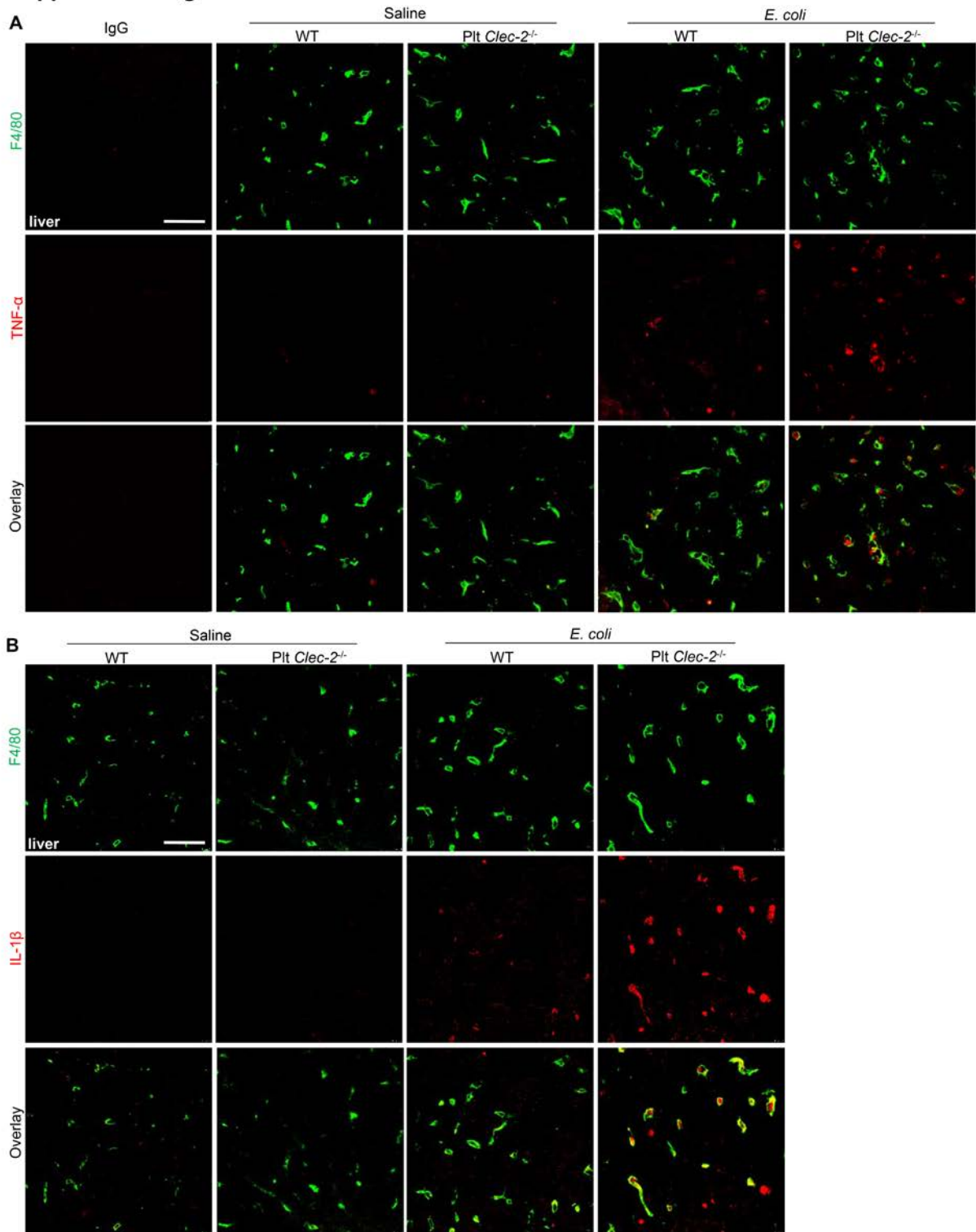
Supplemental Figure 1. Deficiency of platelet CLEC-2 does not affect platelet count and body weight of female mice. Peripheral blood from mice lacking platelet CLEC-2 (Plt *Clec-2*^{-/-}) and their littermate controls (WT) was collected, and platelet count was measured with (A) Hemavet[®] or (B) flow cytometry. (C) Body weight of WT and Plt *Clec-2*^{-/-} mice were measured. Data represent mean \pm sd. n = 15 mice/group. **P* < 0.05. Data were analyzed using an unpaired Student's t test and were representative of four independent experiments.

Supplemental Fig. 2



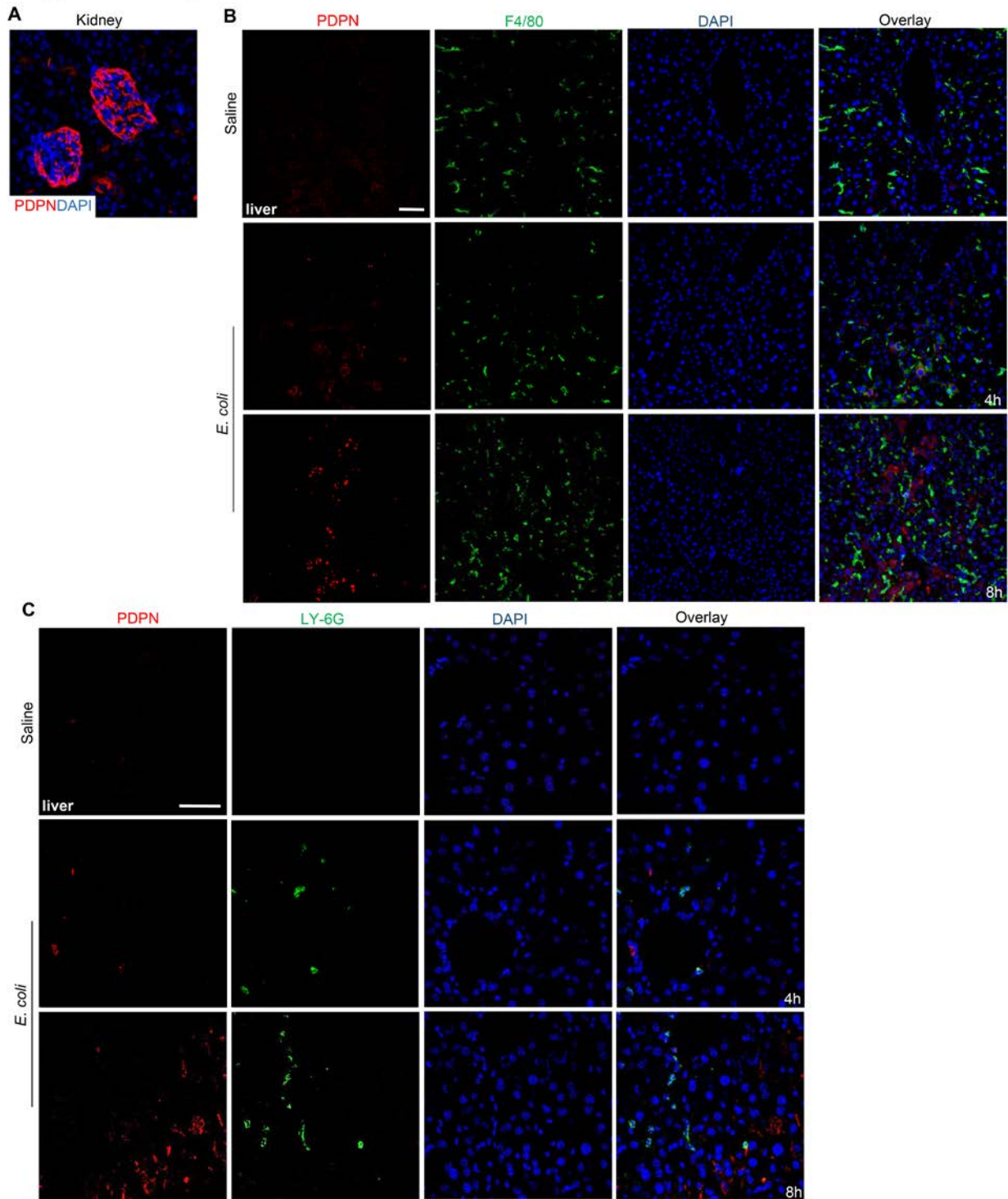
Supplemental Figure 2. Deficiency of platelet CLEC-2 does not affect *E. coli*-induced changes of platelet count and body weight. Female WT and Plt *Clec-2*^{-/-} mice were injected i.p. with a half lethal dose of *E. coli* (2×10^7 CFU/mouse). (A) Peripheral blood was collected before infection and at different time points after infection, and platelet count was measured with Hemavet[®]. (B) Body weight of the same mice was measured. Data represent mean \pm sd. n = 15 mice/group. Data were analyzed using a one-way ANOVA followed by a Tukey's test for multiple groups and were representative of three independent experiments.

Supplemental Fig. 3



Supplemental Figure 3. Platelet CLEC-2 deficiency increases liver inflammation in early sepsis. (A - B) Representative immunofluorescent images of liver cryosections of WT and Plt *clec-2*^{-/-} mice at 8 h post injection of saline or *E. coli*, *n*= 6 mice/group. Scale bar, 10 μm. Data were representative of three independent experiments.

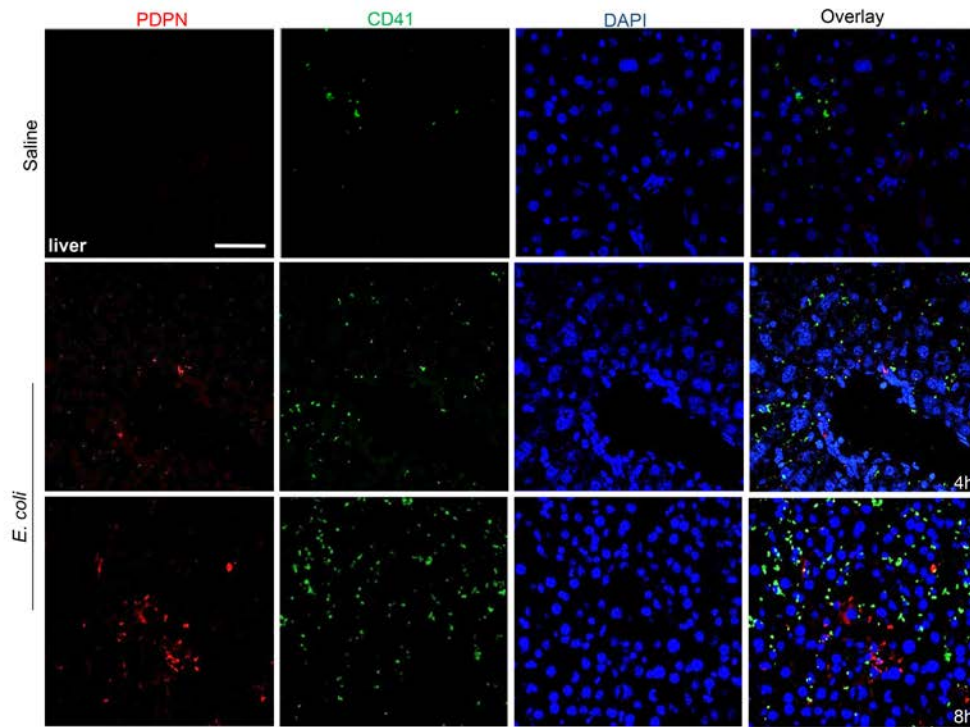
Supplemental Fig. 4



Supplemental Figure 4. Antibodies stain podoplanin in kidney and liver. Representative images of (A) the kidney from healthy WT mice and (B - C) the liver from WT mice at 4 h and 8

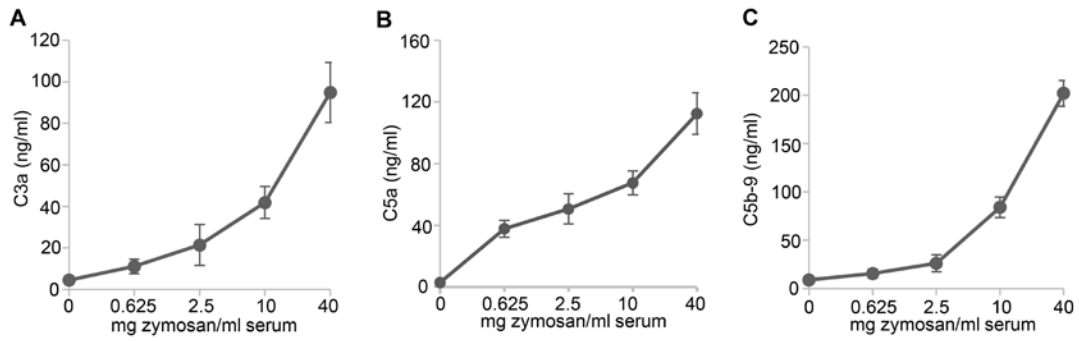
h post injection of saline or *E. coli*. n = 5 mice/group. Scale bar, 25 μm (B) and 10 μm (C). Data were representative of three independent experiments.

Supplemental Fig. 5



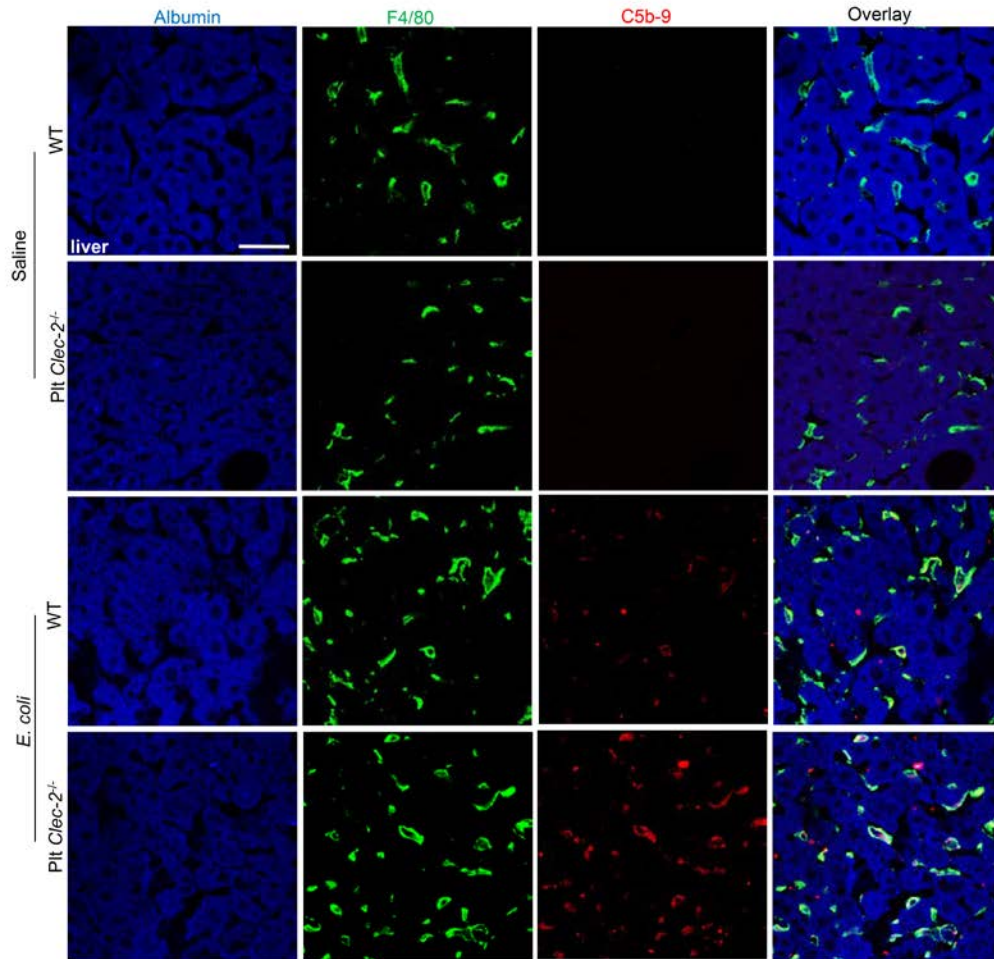
Supplemental Figure 5. Platelet enrichment in septic liver. Representative images of the liver from saline-injected WT mice or WT mice at 4 h and 8 h post injection *E. coli*. n = 5 mice/group. Scale bar, 10 μ m. Data were representative of three independent experiments.

Supplemental Fig. 6



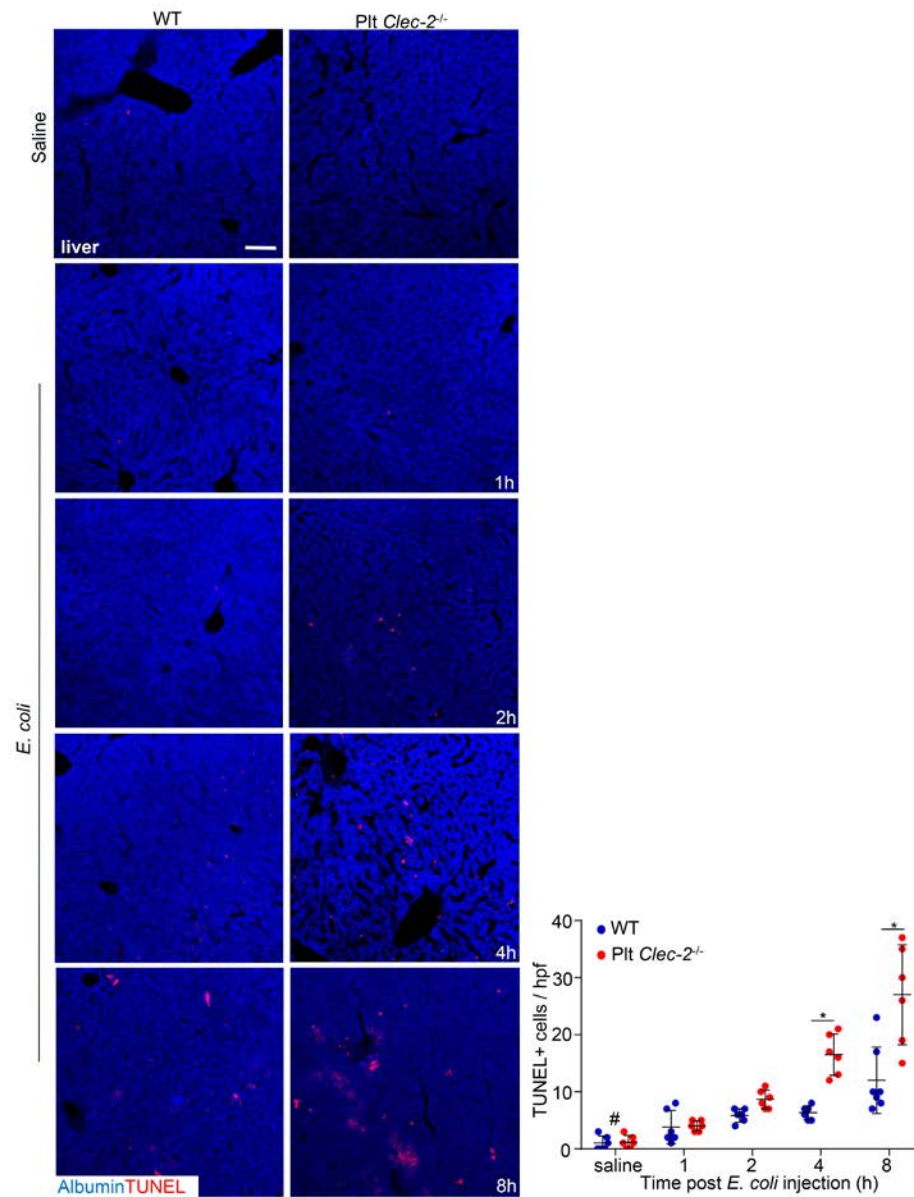
Supplemental Figure 6. Zymosan induces complement activation in a dose-dependent manner. The serum of WT mice was treated with different doses of zymosan and the complement activation products were measured. n = 6 mice/group. Data are mean \pm sd. Data were representative of three independent experiments.

Supplemental Fig. 7



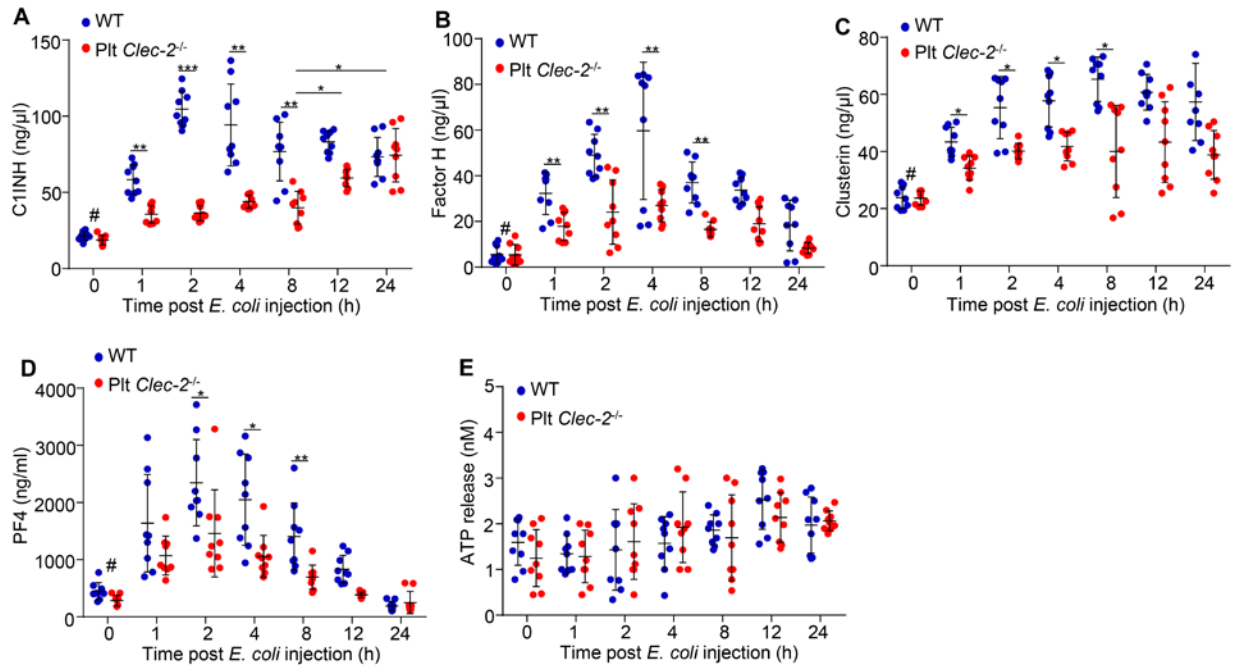
Supplemental Figure 7. Platelet CLEC-2 deficiency increases complement liver attack in early sepsis. Representative images of C5b-9 complex staining of liver cryosections at 8 h after injection of *E. coli* or saline. n = 6 mice/group. Scale bar, 10 μ m. Data were representative of three independent experiments.

Supplemental Fig. 8



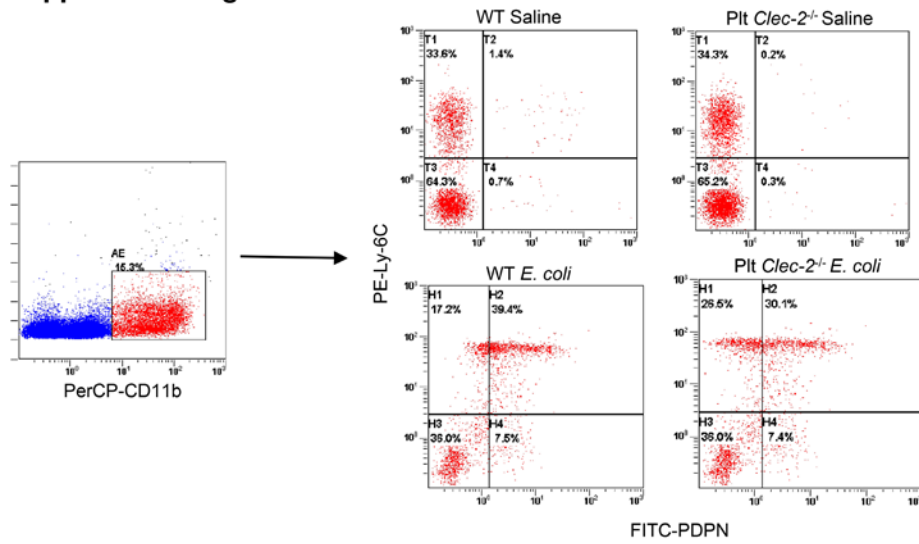
Supplemental Figure 8. Platelet CLEC-2 deficiency increases cell apoptotic death in the liver. Representative images of TUNEL staining of liver cryosections. Bar graphs below were quantifications of TUNEL positive cells. Hpf, high-power microscopic fields. The data are mean \pm sd. n = 6 mice/group. * $P < 0.05$. ** $P < 0.01$. *** $P < 0.001$. Scale bar, 25 μ m. Data were analyzed using a one-way ANOVA followed by a Tukey's test for multiple groups and were representative of three independent experiments.

Supplemental Fig. 9



Supplemental Figure 9. Platelet CLEC-2 deficiency reduces release of complement inhibitors from platelets in early sepsis. (A - E) Plasma levels of different complement inhibitors, PF4, and ATP of WT and Plt *Clec-2*^{-/-} mice with or without *E. coli* injection. The data represent mean \pm sd, n = 9 mice/group. #*P* < 0.05, comparing the sample at 0 h of *E. coli* injection with samples at other time points after *E. coli* infection. **P* < 0.05. ***P* < 0.01. ****P* < 0.001. Data were analyzed using a one-way ANOVA followed by a Tukey's test for multiple groups and were representative of three independent experiments.

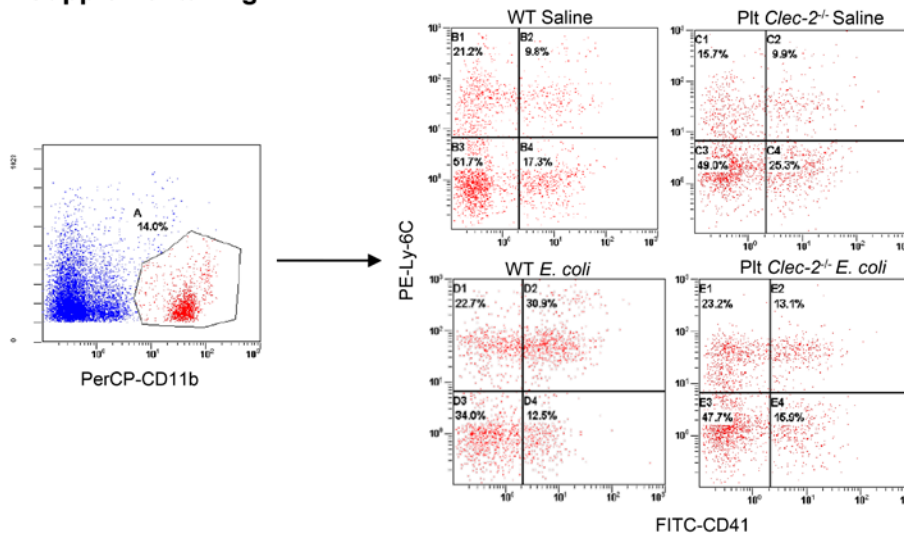
Supplemental Fig. 10



Supplemental Figure 10. Flow chart for measuring podoplanin expression on circulating

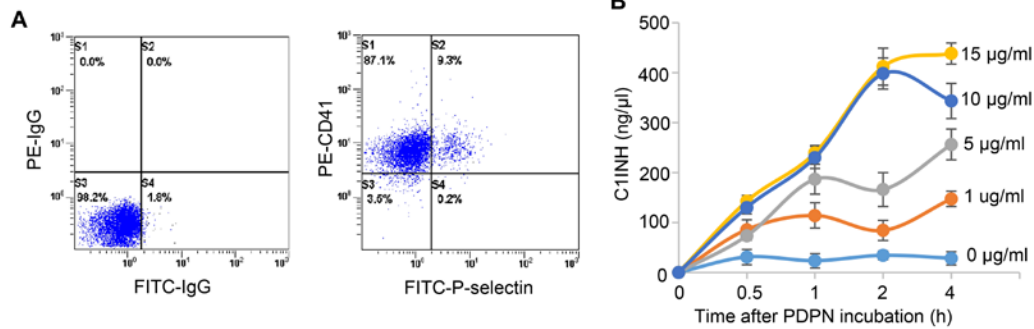
monocytes with flow cytometry. Peripheral blood was collected from WT and Plt *Clec-2*^{-/-} mice at 1 h post injection i.p. of saline or *E. coli* (2×10^7 CFU/mouse). After lysis of red blood cells, the blood samples were incubated with different fluorophore-conjugated antibodies to CD11b, Ly-6C, and podoplanin. White blood cells were distinguished by the size scatter, and then CD11b-positive cell population was selected. The selected cell population was analyzed for expression of Ly-6C and podoplanin. Ly-6C-positive cells, on top of the positive expression of CD11b, were monocytes. In Ly-6C-positive cells, podoplanin-positive cells were further analyzed. The representative data from three independent experiments were shown. $n = 6$ mice/group. Data were representative of three independent experiments.

Supplemental Fig. 11



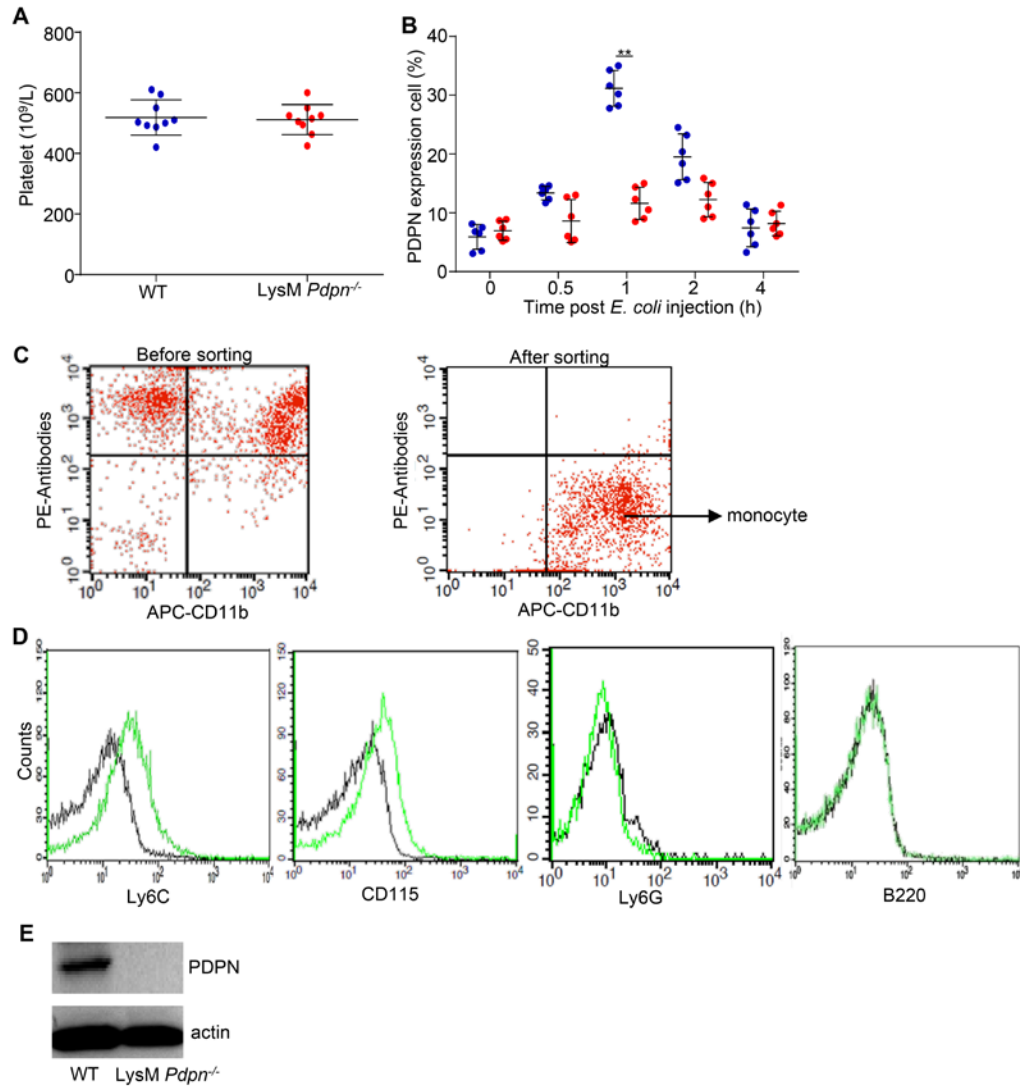
Supplemental Figure 11. Flow chart for measuring the platelet-monocyte aggregate with flow cytometry. Peripheral blood was collected from WT and *Plt Clec-2^{-/-}* mice at 1 h post injection i.p. of saline or *E. coli* (2×10^7 CFU/mouse). After lysis of red blood cells, the blood samples were incubated with different fluorophore-conjugated antibodies to CD11b, Ly-6C, and CD41. White blood cells were distinguished by the size scatter, and then CD11b-positive cell population was selected. The selected cell population was analyzed for expression of Ly-6C and CD41. Ly-6C-positive cells, on top of the positive expression of CD11b, were monocytes. In Ly-6C-positive cells, CD41-positive cells were platelet-monocyte aggregates. The representative data from three independent experiments were shown. $n = 6$ mice/group. Data were representative of three independent experiments.

Supplemental Fig. 12



Supplemental Figure 12. Binding of podoplanin induces a fast and dose-dependent release of complement inhibitor from platelets. Platelets were isolated from peripheral blood of WT mice, and resuspended in modified Tyrode's buffer at a concentration of $1 \times 10^5/\mu\text{l}$. (A) The platelets were incubated with different fluorophore-conjugated antibodies to CD41 and P-selectin. (B) Platelets were incubated with recombinant podoplanin at different doses for different time at 37°C . After removing platelets with centrifugation, the complement inhibitor in the supernatant was measured with ELISA assays. Data are mean \pm sd. $n = 6$ mice/group. Data were representative of three independent experiments.

Supplemental Fig. 13



Supplemental Figure 13. Deficiency of myeloid cell podoplanin abolishes *E. coli*-induced

podoplanin expression on monocytes but not affects platelet count. (A) Peripheral blood

from WT and *LysM Pdpn*^{-/-} mice was collected, and platelet count was measured with

Hemavet[®]. n = 9 mice/group. Data were analyzed using an unpaired Student's t test and were

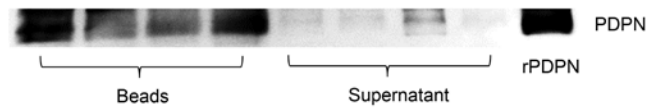
representative of four independent experiments. (B) WT and *LysM Pdpn*^{-/-} mice were injected

i.p. with a half lethal dose of *E. coli* (2×10^7 CFU/mouse). Peripheral blood was collected from

mice at different time points post *E. coli* infection. Podoplanin expression on monocytes was

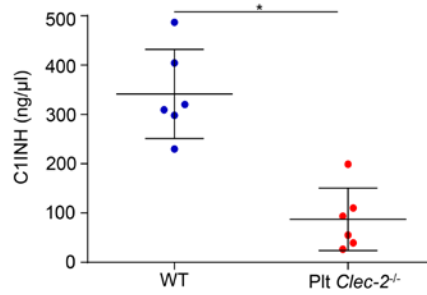
analyzed with flow cytometry. Data represent mean \pm sd. n = 6 mice/group, $**P < 0.01$. Data were analyzed using a one-way ANOVA followed by a Tukey's test for multiple groups and were representative of three independent experiments. (C - D). Primary murine monocytes were purified using flow cytometry with PE-labeled antibodies recognizing CD90, B220, CD49b, NK1.1, Ly-6G surface markers, and an APC-labeled anti-CD11b antibody. The purified monocytes were defined as the PE-negative and APC-positive population. (E) Western blot to probe podoplanin in the lysates of WT and LysM *Pdpr*^{-/-} monocytes. Represent data of three independent experiments was presented. Data were representative of three independent experiments.

Supplemental Fig. 14



Supplemental Figure 14. Protein A/G incubation removes recombinant podoplanin from the platelet supernatant. WT platelets were isolated and resuspended in Tyrode's buffer at a concentration of $1 \times 10^5/\mu\text{l}$. Platelets were incubated with recombinant podoplanin (Fc chimera protein, $10 \mu\text{g/ml}$) for 2 h at 37°C . After spinning down platelets, the supernatant was incubated with protein A/G beads at RT for 1 h. Then the beads were separated from the supernatant by centrifugation. The remained supernatant and the beads were applied on SAS-PAGE gel and the podoplanin was detected by western blot. The representative blot result of three independent experiments was shown. Data were representative of three independent experiments.

Supplemental Fig. 15



Supplemental Figure 15. Measurement of complement inhibitors in the supernatant before the rescue assay. To protect liver function, complement inhibitors were generated by incubating platelets ($1 \times 10^5/\mu\text{l}$ in Tyrode's buffer) from WT and Plt *Clec-2*^{-/-} mice with recombinant podoplanin (Fc chimera protein, 10 $\mu\text{g}/\text{ml}$) for 2 h at 37°C. After removing platelets and soluble podoplanin, complement inhibitors in the supernatant before the rescue assay was measured with an ELISA assay. Data represent mean \pm sd. n = 6 mice/group, * $P < 0.05$. Data were analyzed using an unpaired Student's t test and were representative of four independent experiments.